UNIVERSITY OF BIRMINGHAM
University of Birmingham Research at Birmingham

Evaluation of lateral stability of railway tracks due to ballast degradation

Ngamkhanong, Chayut; Feng, Bin; Tutumluer, Erol; Hashash, Youssef M. A. ; Kaewunruen, Sakdirat

DOI:
10.1016/j.conbuildmat.2021.122342

License:
Creative Commons: Attribution-NonCommercial-NoDerivs (CC BY-NC-ND)

Document Version
Peer reviewed version

Citation for published version (Harvard):
Ngamkhanong, C, Feng, B, Tutumluer, E, Hashash, YMA & Kaewunruen, S 2021, 'Evaluation of lateral stability of railway tracks due to ballast degradation', *Construction and Building Materials*, vol. 278, 122342. https://doi.org/10.1016/j.conbuildmat.2021.122342

Link to publication on Research at Birmingham portal

General rights
Unless a licence is specified above, all rights (including copyright and moral rights) in this document are retained by the authors and/or the copyright holders. The express permission of the copyright holder must be obtained for any use of this material other than for purposes permitted by law.

•Users may freely distribute the URL that is used to identify this publication.
•Users may download and/or print one copy of the publication from the University of Birmingham research portal for the purpose of private study or non-commercial research.
•User may use extracts from the document in line with the concept of 'fair dealing' under the Copyright, Designs and Patents Act 1988 (?)
•Users may not further distribute the material nor use it for the purposes of commercial gain.

Where a licence is displayed above, please note the terms and conditions of the licence govern your use of this document.

When citing, please reference the published version.

Take down policy
While the University of Birmingham exercises care and attention in making items available there are rare occasions when an item has been uploaded in error or has been deemed to be commercially or otherwise sensitive.

If you believe that this is the case for this document, please contact UBIRA@lists.bham.ac.uk providing details and we will remove access to the work immediately and investigate.

Download date: 20. Apr. 2024

Evaluation of Lateral Stability of Railway Tracks due to Ballast Degradation

Chayut Ngamkhanong[1], Bin Feng[2], Erol Tutumluer[2], Youssef MA Hashash[2], & Sakdirat Kaewunruen[1]

[1] Department of Civil Engineering, School of Engineering, University of Birmingham, Birmingham B15 2TT, UK

[2] Department of Civil and Environmental Engineering, University of Illinois at Urbana-Champaign, Urbana, IL, USA

Abstract

Track lateral stability is one of the most critical considerations for safe and reliable railway infrastructures. With increasing exposures to high temperatures globally, a greater expansion in continuous welded rails can induce higher risk of track buckling, especially when track defects exist. In ballasted track structures, ballast layer holds sleepers in place and provides lateral support and stiffness to the track. When ballast deteriorates in services, to what degree a railway track's lateral resistance is compromised has not been fully investigated. Note that the fouling conditions can be due to the accumulation of ballast breakage or outside contamination, such as subgrade intrusion or coal dust, and difficult to inspect in the field. It is evidenced that track buckling can incur even if the railway track and ballast seem to be in a good condition by visual inspection. Therefore, this paper presents a more realistic model to study Single Sleeper (Tie) Push Test (STPT) conditions using the Discrete Element Method (DEM) with the objective to evaluate ballasted track lateral resistance considering different fouling scenarios. The lateral force-displacement curves of sleepers are analysed. The lateral force is derived from the sleeper-ballast contact forces obtained from three main components: sleeper bottom friction, sleeper side friction, and sleeper end force. The fouling conditions are employed by adapting appropriate model parameters in the DEM simulations. The results indicate that fouled ballast can significantly undermine the lateral stability of ballasted tracks by more than about 50%. Track lateral stiffness may be reduced significantly due to fouled ballast layer conditions that cannot be inspected visually in the field. This may reduce track restraint and increase the likelihood of track buckling even though the degraded ballast does not have a direct contact to the sleeper. Finally, the study will enrich the development of inspection criteria for ballast lateral resistance and support conditions, improve safety and reliability of rail network, and mitigate the risk of delays due to track buckling leading to unplanned maintenance.

1. Introduction

Railway track buckling has become a serious concern due to higher than average summer temperatures observed globally and the increasing risk of track buckling noted around the world [1]. The increase in global temperatures can induce higher rail temperatures and build up the compression force in the continuous welded rail (CWR). Although CWR provides a smooth ride and has lower maintenance cost, CWR still suffers from drawbacks in which the track tends to buckle easily when the rail temperature reaches a certain limit. Many research studies have indicated that track buckling has been one of the major causes of train derailments associated with huge losses of life and assets [2, 3]. It has been found that the track components developing resistance to rail buckle are the sleeper and the supporting ballast. Lateral ballast resistance not only resists track buckling but also helps to maintain lateral track alignment which is one of the reasons for the lateral force in the rails. Ballast providing lateral resistance can be stated as the most significant factor to resist the buckling forces during the expansion of rail. Lateral resistance of ballast consists of three main components: bottom friction of sleeper, side friction of sleeper and ballast shoulder restraint, as shown in Figure 1. The resistance force is calculated from the summation of ballast-sleeper contact force in lateral plane to encounter the sleeper movement.

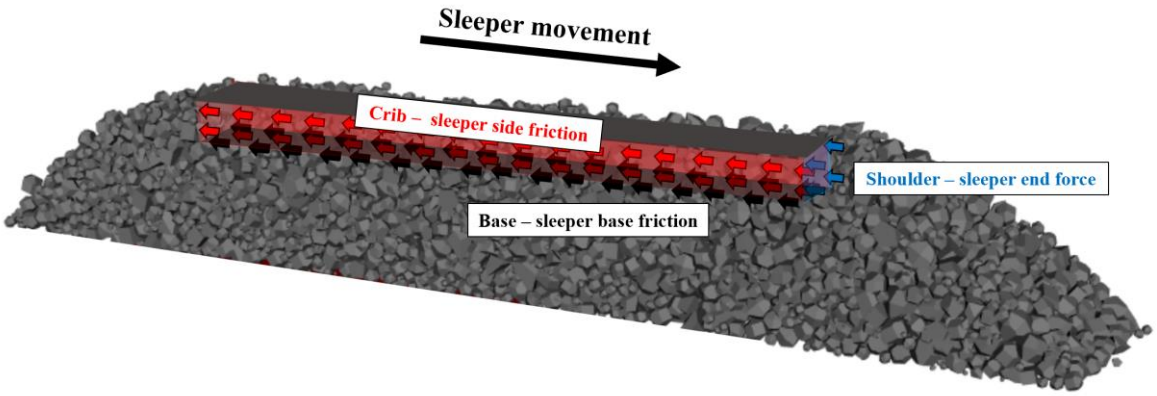

Figure 1. Contributions of different frictional components.

As evidenced in the UK and worldwide, railway track buckling can still occur even if the railway tracks are fully supported and the ballast layer seems to be in good condition by visual inspection. In fact, degraded ballast particles and the accumulation of ballast breakdown or outside contamination, such as subgrade intrusion or coal dust, often may not be seen visually [4, 5]. Their presence undoubtedly would have a negative impact on the vertical stiffness of the railway tracks and cause potential track geometry defects. No quantifiable data currently exist on the extent degraded ballast could influence the lateral stiffness of ballasted track and what percent the fine particles generated in a fouled ballast would decrease the lateral support through direct contact with the sleeper. Accordingly, there is a need to study and quantify the effect of the progressive degradation of ballast influencing lateral resistance by properly considering the contributions of the different frictional components in a ballasted track.

According to previous research on track buckling simulations using the Finite Element Method (FEM) [6-8], railway tracks were mostly modelled using a series of beams and springs to represent track components. The nonlinear tensionless springs of ballast have been applied at the sleeper ends to represent the actual behaviour of ballast. The elastoplastic curve of lateral resistance has been also used in modelling of track buckling. It is noted that the properties of lateral springs of ballast connected to sleepers are derived from the contact force between sleeper and ballast, and displacement of sleeper subjected to lateral load from Single Sleeper (Tie) Push Tests (STPTs) [9, 10]. This method has been proven to be the most suitable method to quantify the lateral resistance of tracks recommended by AREMA [11]. There has been much research conducted on the STPTs of sleepers to obtain the lateral resistance-displacement curve of sleepers for ballasted track. This method can measure the lateral resistance of sleeper-ballast interaction.

To model the STPT, researchers considered ballast layer as a continuum model represented by a homogeneous material consisting of connected uniform elements of infinitesimal size [12]. The three-dimensional FEM models were developed for sleepers embedded in the homogeneous ballast [13, 14]. The friction coefficient between sleeper and ballast was then varied to study the lateral resistance of ballasted track. The results showed good trends and were reasonable. However, some of the modelling aspects, such as friction and boundary conditions, in these previous studies were mostly based on certain assumptions which made the results often questionable. Most importantly, it is a wrong assumption to treat railway ballast as a continuum due to the particulate nature of a ballast layer assembly which, in fact, consists of aggregate particles, each approximately 40-75 mm [15] in size. A more realistic numerical simulation approach has been the Discrete Element Method (DEM), which is nowadays widely used for simulating load-deformation behaviour of ballast layer granular materials. DEM for granular material was first introduced for rock and soil particles [16]. This approach is a numerical method for computing the deformations of individual particles with interactions in a granular assembly. DEM can provide insight into the micro-mechanical behaviour of railway ballast. Recent research studies have proposed to use different DEM approaches to analyse the lateral resistance of ballasted

track including STPT simulations and considered different types of ballast particles used as discrete elements [17-21].

The lateral resistance of ballasted track is commonly reduced with usage due to long-term degradation, maintenance activities and ballast disturbance. There are several methods that can potentially improve the lateral resistance of ballasted track such as using different shapes of sleepers [20, 22], ballast gluing [23], ballast reinforcement [24], and track maintenance or renewal. The effects of ballast particle shapes and tamping activity on the lateral stability of ballasted track have also been studied [25]. Tamping activities have been found to impact lateral resistance by loosening the compacted state of the ballast layer. It is also known that angular ballast particles have higher shear resistance than rounded ones and the ballast degradation is directly related to the crushed stone type aggregate source and particle morphology [26]. The shapes of deteriorated ballast particles tend to become more rounded than sharp cornered. The round gravel ballast can reduce the lateral resistance by about 30-35% [27].

Railway track is progressively degraded with usage making the improvement of ballasted track necessary. Most importantly, lack of ballast support can significantly undermine the capacity of railway track [28, 29]. For instance, in a track which is in poor condition, large voids and gaps can easily be observed between sleepers and the ballast, usually caused by the wet track beds (highly moist ground) from natural water springs or poor drainage. The strength and drainage aspects of ballasted tracks are compromised due to the increasing level of ballast fouling. This leads to larger particle movement resulting in more severe loss of support conditions. Since it is not clear to what extent progressive ballast degradation and fouling may decrease lateral resistance of ballasted tracks, the research study described in this paper was therefore intended to quantify major contributions of frictional components of a sleeper on track lateral resistance through a realistic DEM modelling approach for ballast behavior.

This paper presents results of DEM simulations of push tests of single timber and concrete sleepers by considering different levels of fouling within the ballast depth profile. The study compares the effects of progressive ballast fouling conditions that start with accumulating finer particles from the bottom and consider different heights all the way to the top to finally represent the full-depth fouled ballast profile. Such effects of ballast condition and vulnerability influencing track lateral resistance are quantified through DEM simulations. The results presented are discussed in relation to allowable magnitudes of rail buckle forces that can be resisted and safe temperatures that the tracks can withstand under these ballast conditions. The findings presented are intended to help track engineers to better evaluate how different fouled ballast conditions can be related to performance and hence to develop inspection criteria related to ballast layer maintenance and renewal associated with the level of ballast degradation.

2. Lateral resistance of ballasted tracks

Researchers in the past have conducted both numerical and experimental studies to obtain the lateral resistance of track. As for numerical, different methods have been applied for quantifying lateral resistance force through FEM and DEM approaches considering different contact parameters and types of particle shapes. Several parameters were assumed especially for FEM [13, 14] and DEM spherical shapes [18]. In addition, spherical clump and polyhedral particles have been previously used for STPT simulations in DEM [17, 19-21]. These studies mostly considered the tracks when ballast was well compacted and the ballast shapes were assumed as clumps of spherical particles. Both the textured sleepers [13, 17] and ladder sleepers [22] were shown to improve the lateral resistance of ballasted track. Further, many researchers also studied the effects different dimensions and profiles of ballast layer [19, 30]. It was found that the frictional components of the sleeper bottom and sides had a major role in determining track lateral resistance. Also, widening the ballast shoulder could help increase the lateral resistance. Nonetheless, only few studies using DEM focused on the effect of ballast particle shape, i.e., the angularity [17]. It was found that ballast with angular aggregates provided better shear resistance than ballast with round particle shapes, however, the results were not fully indicative since

only sleeper base friction was considered [17]. Different geometries of ballast layer were factored only for the ballast thickness and shoulder length [19].

Measurements for lateral resistance have been widely conducted through field experiments [9, 10, 19, 20, 31-33]. Although the STPTs were carried out in both laboratory and field experiments, it was found that the lateral resistance of track in the laboratory experiments was generally less than that in the field due to the different compaction levels [32]. Note that the lateral resistance in the field tends to be larger since the tracks have been operated at some point before the tests take place. Most of the previous studies with field experiments focused on the effects of sleepers on lateral resistance of ballasted track with clean ballast. The methods of improving lateral resistance using more detailed sleeper geometries and dimensions, such as in the types of frictional sleepers, ladder sleepers, etc., were studied in the field. No doubt these different sleeper types and features could significantly improve the lateral stiffness of railway track [21, 22, 24, 34]. As for the ballast layer contribution, some kind of ballast particle gluing has been applied to railway tracks to improve the lateral stability [23, 24]. Moreover, different types of ballast materials, i.e., limestone and steel slag, with a similar gradation were also considered in the field measurements [35], and the steel slag was found to provide better lateral resistance than limestone ballast due to its higher bulk specific gravity.

A recent European review provided benchmarked STPT results for the lateral resistance of ballasted track during different ballast construction and in-service stages [27]. Based on this benchmarking, Figure 2 presents a comparison of the results from various STPT research studies for mono-block concrete sleepers only. The different track conditions and ballast construction and in-service stages correspond to unballasted track or lying free, loosely filled track, tamped, and lined track, dynamically stabilised track, and well filled and fully stabilised track according to [27]. The typical values of lateral resistance of ballasted track with concrete sleeper are presented at the sleeper displacement of 2 mm, which tends to be over the yielding point [27]. Note that this yielding point is when lateral stiffness is reduced after the sleeper displaces and was reported in the literature to be between 0.5 and 2 mm. The lateral contact force only has a very slight change and is likely to be constant after yielding point or elastic limit. Figure 2 indicates the lateral resistance of ballasted track to fall within the stage of loosely filled and tamped and lined track when track buckling might occur in reality.

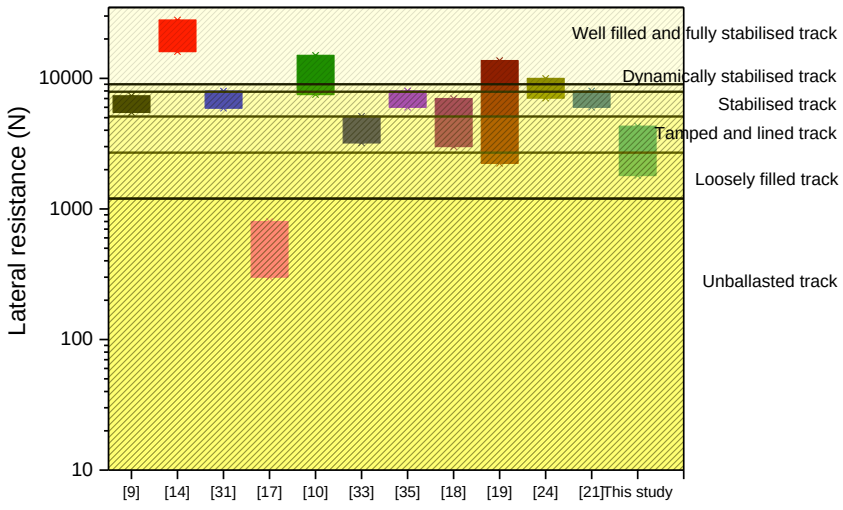

Figure 2 Lateral resistance of ballasted track at sleeper displacement of 2 mm with benchmarked values [27].

3. Discrete element modelling

This paper considers the cross-section of typical single ballasted track with the mono-block timber and concrete sleepers laid on ballast layer. Timber sleeper with dimensions of 250x150x2600 mm and concrete sleeper with dimensions of 260x235x2600 mm are separately constructed on top of a 300 mm thick ballast layer. The material properties and dimensions of sleepers are presented in Table 1. The physical models of the ballast layer geometry were first constructed without ballast shoulder and crib as shown in Figure 3. The dimensions of the established ballast layer model are presented with sleeper dimensions. Full width of the track is modelled with 400 mm wide ballast shoulders and a 1:1.5 shoulder slope. The longitudinal dimension of the track is 600 mm which is equal to the typical sleeper spacing. Hence, the model boundary area is set as 600 mm in length and 4600 mm in width.

Table 1 Sleeper characteristics.

Sleeper types		Value	Unit
Timber sleeper (Hardwood)			
Density		1100	kg/m^3
Elastic modulus		16000	MPa
Poisson's ratio		0.25	
Dimension	Length	2600	mm
	Height	150	mm
	Width	250	mm
Concrete sleeper			
Density		2740	kg/m^3
Elastic modulus		37500	MPa
Poisson's ratio		0.2	
Dimension	Length	2600	mm
	Height	260	mm
	Width	235	mm

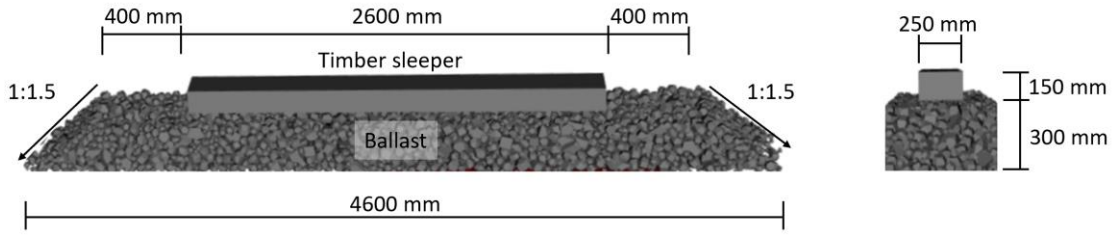

(a)

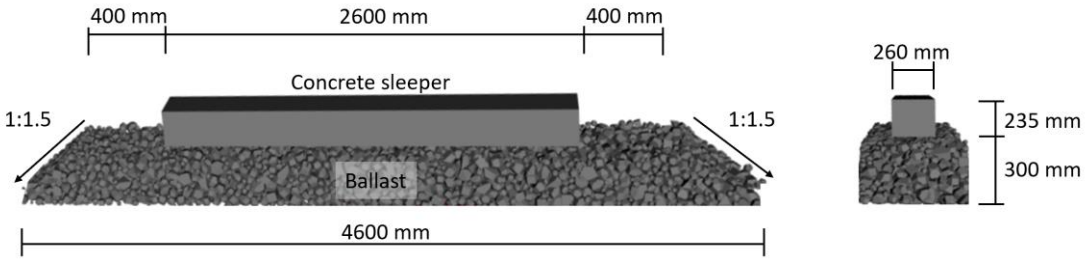

(b)

Figure 3. Sleeper and ballast layer geometry studied: (a) timber sleeper, (b) concrete sleeper.

The DEM models were then extended for sleeper with full ballast components including ballast crib and shoulder. This study considers the following three ballast fouling conditions within the layer depth profile: (1) 100-mm fouled layer at the bottom, (2) 200-mm fouled layer at the bottom, and (3) full-depth fouled ballast layer, as shown in Figure 4. It was assumed that the breakdown of ballast material due to the load from the sleeper generated ballast fines which migrates from top to bottom and starts to accumulate at the bottom of the ballast layer [5]. Note that this may not be the case if soft subgrade causes mud pumping and subgrade soil fines intruded may be collected and observed at any depth profile in the ballast layer [36, 37]. This phenomenon is represented in the DEM simulations here with the whole ballast layer fouled. The details of the progressive ballast fouling conditions with fines accumulating from bottom to top, i.e. most observed ballast material breakdown, are explained in the next section.

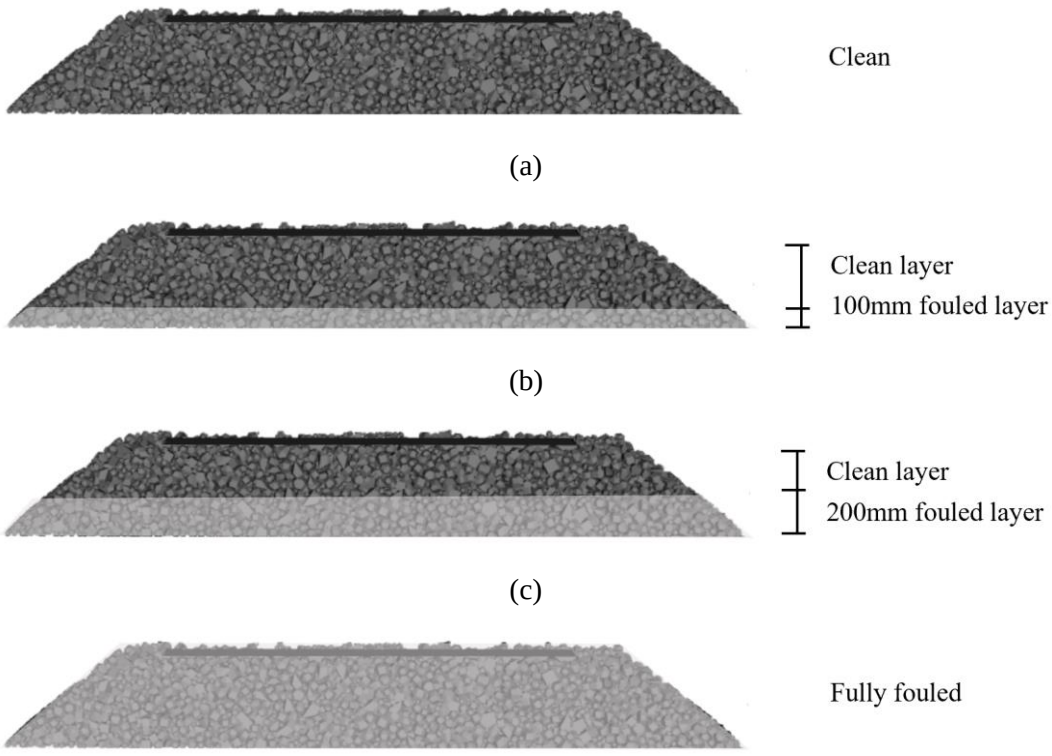

Figure 4. Schematic view of a) clean ballast layer b) 100 mm fouled ballast layer c) 200 mm fouled ballast layer e) fully fouled ballast layer.

To create realistic shapes of railway ballast crushed aggregate particles, polyhedral elements need to be used in ballast DEM simulations. This approach can generate non-spherical particles and potentially provide better insight into interparticle contacts by properly accounting for corners and sharp edges of the particles, which are essentially needed to simulate correctly dilatancy angles in angular particle assemblies. In this study, the ballast shapes and their morphological properties are analysed using the Enhanced University of Illinois Aggregate Image Analyzer (E-UIAIA) [38]. The E-UIAIA is the imaging technology to capture the realistic 3D shapes of ballast particles from three orthogonal views to quantify detailed shapes and measurements of each particle including surface texture (ST) index,

angularity index (AI) and flat and elongated (F&E) ratio. The ballast particles obtained by E-UIAIA were imported to BLOKS3D DEM software developed and extensively used at the University of Illinois at Urbana-Champaign in the last three decades [39, 40]. Note that AI simply presents an average of the Angularity values of all the particles weighted by the particle weight, which measures overall degree changes on the boundary of a 2D particle silhouette. The flat and elongated (F&E) ratio illustrates the ratio of the longest dimension of the particle to its shortest dimension from the three orthogonal views; for each 2D silhouette the shortest Feret dimension is perpendicular to the longest Feret dimension.

The shapes and geometric properties of the ballast particles used in this study are presented in Table 2. The percentages of particles and the average AI values used in this simulation are also presented. It should be noted that even though the particles are randomly generated, the ballast proportions of all cases are constantly controlled to make the DEM models consistent. The proportions and AI of each particle are calculated using the E-UIAIA to match the field-collected ballast sample database [29]. The average AI is calculated by taking a weighted average of the AI of each ballast shape, weighted by the percentage of number of particles. It should be noted that the average AI is around 430 which is considered as a low angularity value mostly representing more of round shaped particles [17]. This generally presents the ageing of railway ballast with the particles having less angularity. Moreover, air voids considered is roughly 38% of the volume of the ballast layer and thus making the ballast layer in somewhat loose condition since the expected air voids for compacted ballast should reach 35% in the field [36]. The particle distribution curve of the ballast sample studied herein is shown in Figure 5. The ballast gradation conforms to the American Railway Engineering and Maintenance-of-Way Association (AREMA) No. 24 standard specification.

Table 2. Imaging based shape indices of ballast particles used as discrete elements in DEM simulations.

No	Ballast shape	Percentage of number of particles (%)	Angularity Index (AI)	Flat & Elongated ratio (F&E)
1		3.56	720	1:1
2		10.20	570	1:1
3		19.30	448	1:1
4		66.94	390	1:1
		Average	430	1:1

The DEM model parameters consist of normal stiffness, shear stiffness and surface friction. The DEM model parameters used are presented in Table 3. Note that the model parameters used for ballast have been validated with the previous experimental results based on direct shear and triaxial tests [41]. Accordingly, the surface friction angle between two individual ballast particles is set as 31 degrees. Note that these DEM model parameters in Table 3 gave good predictions when compared to the experimental results obtained in the laboratory [36]. In terms of contact between sleeper and ballast, the surface friction angles for both timber and concrete sleepers to ballast are assumed equally to be 30 degrees, which is a value obtained previously for contact between concrete sleeper and ballast. It should be noted that the surfaces of concrete sleepers are relatively smooth in comparison to timber sleepers. This may slightly affect the results on the contact between sleeper bottom and ballast. However, the

effect is probably negligible since the total lateral resistance increases by about 5% when the surface friction angle increases from 30 to 40 degrees. Accordingly, the surface friction angle of 30 degrees is used in this study for both the timber and concrete sleeper cases.

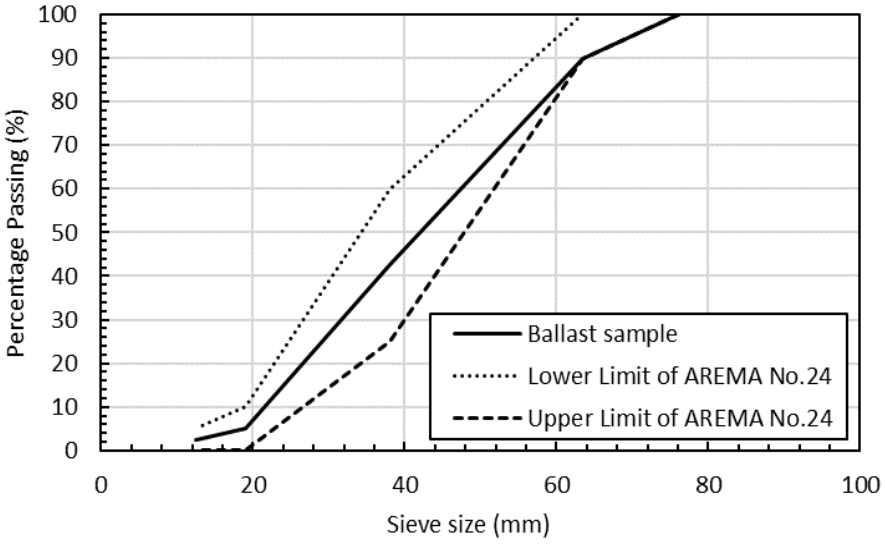

Figure 5**. Ballast particle size distribution conforming to AREMA No. 24 standard ballast specification.**

Table 3 DEM ballast layer simulation model parameters.

Parameters	Value	Unit
Normal stiffness	20	MN/m
Shear stiffness	10	MN/m
Surface friction angle (for clean layer)	31	°
Surface friction angle (for fouled layer)	27	°
Global damping	0	
Contact damping	0.4	

For the ballast layer preparation, 5 infinite planes, consisting of bottom, left, right, front, and back, are first built to create the global boundary area to prevent the ballast particles going through. Then, inclined rigid blocks are used to provide the layer features and dimensions (shown in Figure 3) for the constructed ballast with the indicated shoulder slope. For the clean ballast, approximately 12,805 ballast particles are generated and randomly dropped into the boundary area to generate the ballast layer. The particles above the target height are removed and the non-deformable compaction plate is then pushed downward on top of the particles applying the normal pressure of 100kN to compact the ballast layer until it reaches the target void ratio and no particle movement observed. Sleeper, which is modelled as a non-deformable master block, is applied on top of the ballast layer. It should be noted that the flexural behaviour of the sleeper is not considered so that the non-deformable master block can be properly considered in this study. Two types of sleepers (concrete and timber) are considered.

Next, the STPT test is conducted first for ballasted track with no ballast shoulder and crib. As for the layer with ballast crib and shoulder, more ballast particles are added later to generate ballast shoulder and crib. It is noted that the ballast is randomly dropped so that the ballast particles, which have the

centroid over the depth of sleeper, are removed. Thus, ballast crib and shoulder height are set as a depth of sleeper. Also, the height of ballast shoulder above the sleeper top does not play a significant role in influencing the lateral resistance as evidenced in previous studies [14, 31]. After layer preparation, a transverse velocity of 0.5 mm/s is applied to the sleeper. The sleeper is displaced laterally for about 3 mm. It should be noted that after reaching this point, the slope of force-displacement representing lateral stiffness is almost constant. The resistance forces are calculated from the total contact force between sleeper and ballast against the movement of sleeper combining three different locations: sleeper bottom, sleeper crib, and sleeper end force.

Ballast fouling mechanism

Generally, ballast is progressively fouled over time as the voids among particles are filled with finer materials. The major source of ballast fouling is ballast breakdown, which is about 76% of all sources as found in North America [42]. Other sources are infiltration from underlying layers and ballast surface which make up 13% and 7%, respectively. They are followed by subgrade intrusion (3%) and sleeper wear (1%) [42]. Ballast fouling has been emphasized to greatly undermine the stability and strength of railway track by many researchers [36, 43]. Further, ballast fouling may cause drainage issues in ballasted track since the voids are filled up and water is blocked, leading to higher levels of moisture accumulating in the track substructure [44]. Figure 6 presents the ballast fouling phases and their mechanisms. Phase 1 presents clean ballast where each particle is in contact with others. Since there are voids between particles, finer materials easily fill those voids. The contacts between particles are still maintained while the contact strength can be reduced significantly. In phase 3, the ballast is heavily fouled leading to the elimination of particle contact. Note that many of the ballast particles shown in Figure 6 phase 3 are not as large as in the case of clean new ballast composition due to the significant breakdown and the movement of each particle is constrained by finer materials filling the voids. In this situation, the ballast undoubtedly requires improvement and maintenance. This normally happens when the percentage of fouling particles in the ballast layer is higher than 50% [45].

a) Clean ballast (Phase 1) b) Partially fouled ballast (Phase 2) c) Heavily fouled ballast (Phase 3)

Figure 6. Critical ballast fouling phases [46].

According to the previous experiments [46], three types of fine materials: coal dust, plastic clayey soil and mineral filler were added to the dry and wet ballast conditions. Coal dust was chosen as the fouling agent due to being commonly found in coal lines with its poor mechanical properties and it was reported to cause the most significant decreases in aggregate assembly strength compared to other fouling agents [41].

In DEM simulations, there are two approaches to represent the fouled ballast conditions. The direct approach is used to apply the new size distribution of fouled ballast so that more particles are represented. This approach may take longer computational time and larger memory consumption due to the larger number of particles included in DEM simulations. Another approach is to assume fouled ballast will still have large aggregate particles contacting each other, such as in the case of new ballast

gradation, but individual particles having much lower surface friction angles, which is adopted here as the modified DEM model parameter. This approach is based on previous experiments using coal dust as a fine material in direct shear tests [41]. It is noted that the coal dust acts as a lubricant which can reduce the friction between particles and assigning a lower surface friction angle between two discrete ballast particles/elements in contact, which is the approach adopted herein for DEM simulations. This method still allows dealing with new ballast type uniform gradations having much fewer particles than for degraded ballast particle size distributions and provides better simulation time. However, this is based on the assumption that the void ratio and compaction characteristics are completely similar in both clean and fouled ballast conditions while, in fact, when ballast layer is fouled, the void volume must be reduced [36].

For the fouled ballast DEM simulations shown in Figure 4b, 4c, and 4d, the surface friction angle is reduced to 27 degrees in the fouled layer to match the laboratory results for fouled ballast in case of 15% dry coal dust fouling as resulted in [41]. The normal and shear contact stiffness values are kept the same based on the assumption that the coal dust does not greatly affect the contact stiffness. As for the simulation approaches for partially fouled conditions, the ballast layer can be divided into two layers: fouled and clean layers. The fouled ballast particles with a surface friction angle of 27 degrees are firstly dropped in the boundary area. The particles over the target of fouling level are then removed to generate an exact depth of fouled ballast layer. After that, the second layer, which represents the clean ballast layer, is made by dropping the particles with a surface friction angle of 31 degrees. These cases represent the partially fouled conditions where fine aggregates are accumulated at the bottom layer. Lastly, the completely fouled condition is taken into consideration by reducing the surface friction angle on the whole ballast layer (see Figure 4d). The simulation approaches of this case are like that for completely clean layer but with a surface friction angle of 27 degrees.

4. Results and Discussion

The lateral resistance of ballasted track with timber and concrete sleepers are shown in Figures 7 and 8, respectively. The lateral force is computed by the summation of contact forces between sleeper and ballast in transverse direction. It should be noted that the raw data results have been smoothened using an adjacent-averaging method to remove the spikes from signals. It is well known that adding ballast shoulder and crib can significantly increase lateral resistance of ballasted tracks with both timber and concrete sleepers. A similar trend of lateral force-displacement of sleepers can be found in both timber and concrete sleepers. The slope of this curve presents the lateral stiffness of ballasted track due to sleeper-ballast contact. It is noted that the curves are likely to be bilinear which can be fit to the original ones. The lateral resistance increases as the sleeper displacement increases until reaching a certain value or displacement limit. At that certain point, sleeper displacement yields, and lateral stiffness tends to be reduced. From the results presented in Figure 8, the lateral force at 2mm concrete sleeper displacement is about 3.8kN. According to the benchmarking models [27], it implies that the lateral resistance of concrete sleeper cases in this study matches well and falls within the loosely filled (lateral resistance < 2.5kN) and tamped stages (lateral resistance < 5.1kN) as expected in this study. This value is lower for timber sleeper to be just above 3 kN (see Figure 7).

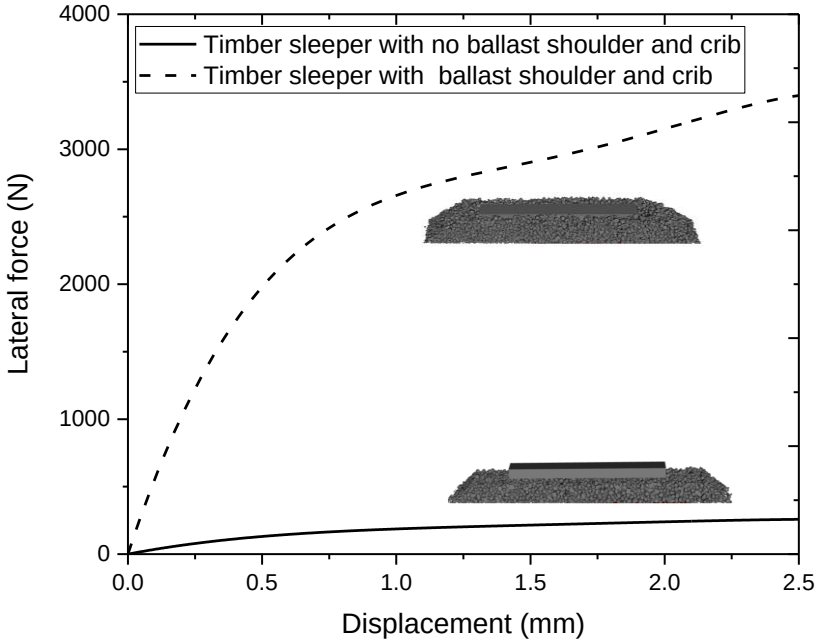

349

350 **Figure 7. Lateral force - displacement graph for timber sleeper.**

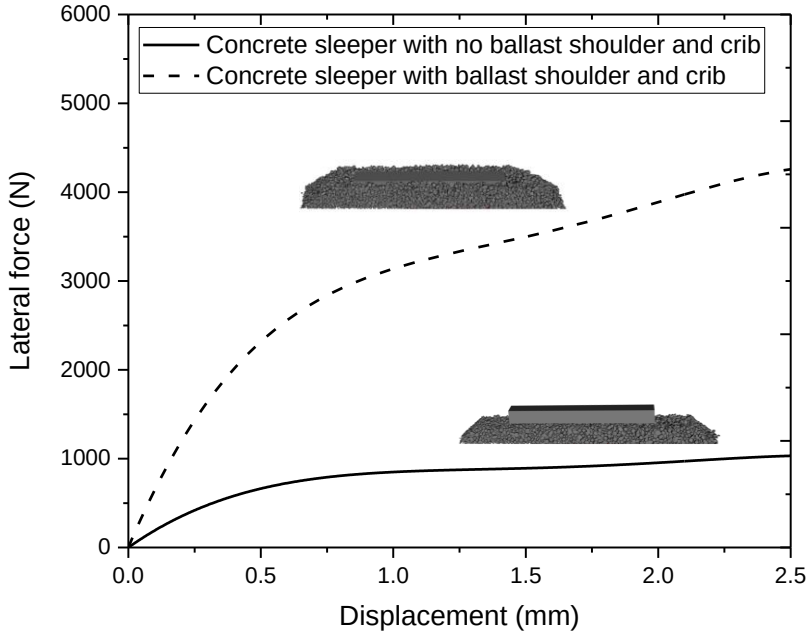

351

352 **Figure 8. Lateral force - displacement graph for concrete sleeper.**

353

354 The increases in lateral resistance after the addition of ballast shoulder and crib are presented for timber
355 and concrete sleepers in Figure 9. This indicates that adding a ballast shoulder and crib can significantly
356 increase the lateral resistance even though the sleeper displacement has reached a certain yield point.
357 After this certain sleeper displacement, the ballast and crib can still improve the lateral resistance of

ballasted track but in lower rate. The lateral stiffness after this yield point depends on the ballast shoulder and crib properties. However, the results for both timber and concrete sleepers tend to be similar in magnitudes with a slight difference which may be due to the effect of surface friction angles that are assumed to be the same for both cases.

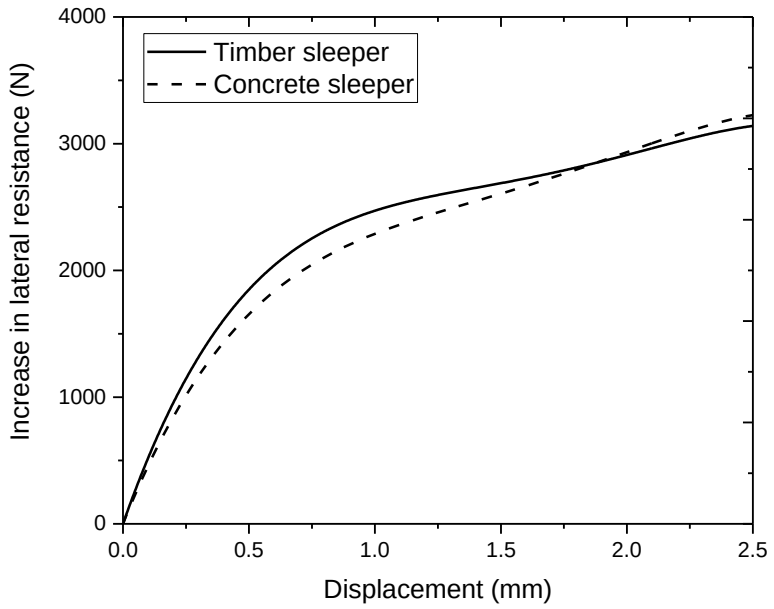

Figure 9. Increase in lateral resistance after adding ballast shoulder and crib.

The lateral resistance ratio over sleeper displacement of timber sleeper to concrete sleeper is presented in Figure 10. It is shown that, as for ballasted track with no ballast shoulder and crib, lateral resistance of ballasted tracks with timber sleepers is about 20-30% of that of tracks with concrete sleepers as the sleeper weight and shape are changed. It is noted that this is directly related to the weight and shape of a sleeper. While the ratio of lateral resistance of ballasted track with ballast shoulder and crib is between 0.80-0.85. This is because the sleeper side friction and ballast shoulder also help to increase the lateral resistance and these parts are not influenced by sleeper weight.

The lateral resistance values of ballasted tracks under fouled conditions are presented for timber and concrete sleepers in Figures 11 and 12, respectively. The displacement limit, which is also known as the yield point, is established between 0.5mm and 1mm. It is observed that the lateral resistance is gradually reduced when the fouled layer becomes thicker and the ballast fouling tends to reduce not only lateral resistance but also the lateral initial stiffness. The initial stiffness is decreased as the fouled ballast thickness is increased.

The reduction of lateral resistance of ballasted tracks are presented in Figure 13. This reduction of lateral resistance is calculated based on the difference between the lateral resistance of track with clean ballast and that with different fouled ballast layers ($\frac{R_{clean}-R_{fouled}}{R_{clean}} x100$, where R is the resistance). Note that the resistance is measured when the sleeper displaces by 2mm. The thicker the layer of fouled ballast, the lower is the lateral resistance. For the timber sleeper, the reduction rates are 13-15%, 21-25%, and 38-48% for tracks with the fouled ballast thicknesses of 100mm, 200mm, and 300mm, respectively. While the reduction rates of tracks with concrete sleepers tend to be higher than timber sleepers since 17-21%, 23-38%, and 39-64% reductions are observed for tracks for the fouled ballast thicknesses of

100mm, 200mm, and 300mm, respectively. Tracks without a ballast shoulder and crib are likely to be more sensitive since reduction rates in lateral resistance will be higher than those with ballast shoulder and crib.

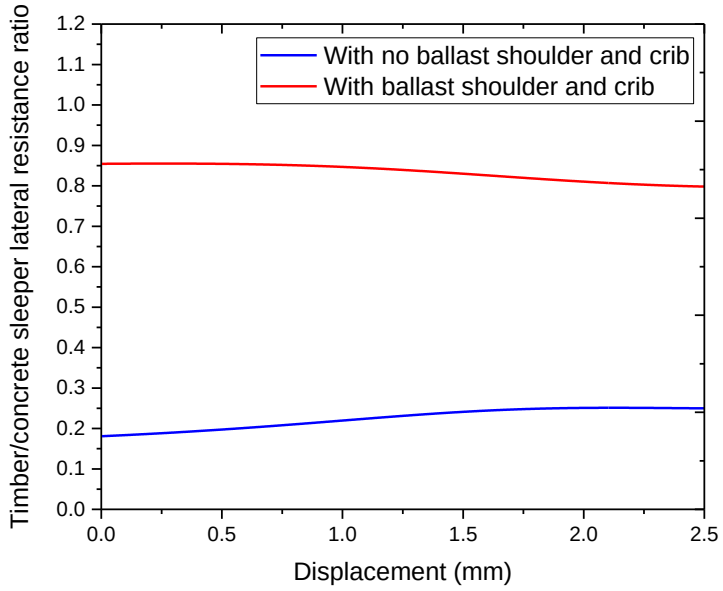

Figure 10. Timber/concrete sleeper lateral resistance ratio.

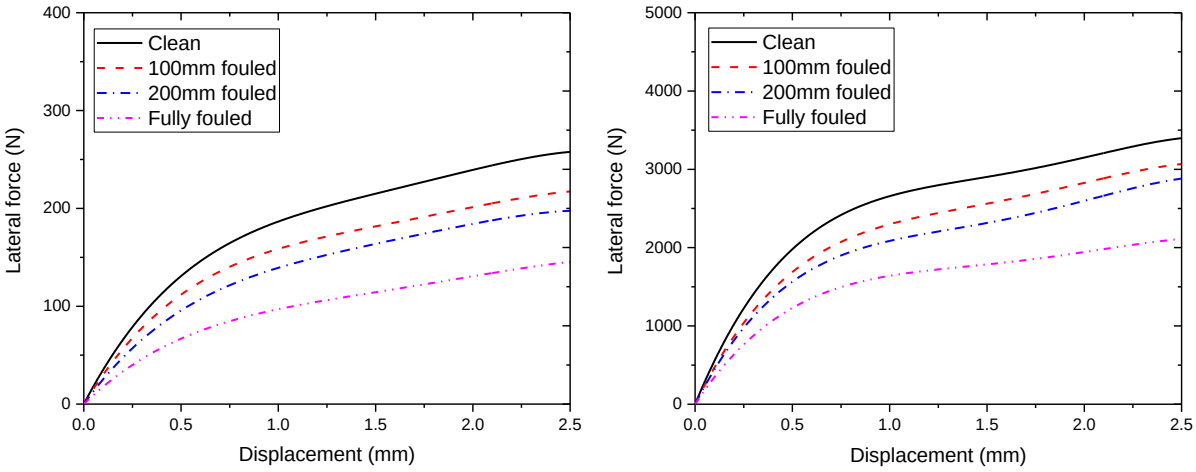

(a) Timber sleeper with no ballast shoulder (b) Timber sleeper with ballast shoulder

Figure 11. Lateral force - displacement graph for timber sleeper considering fouled ballast.

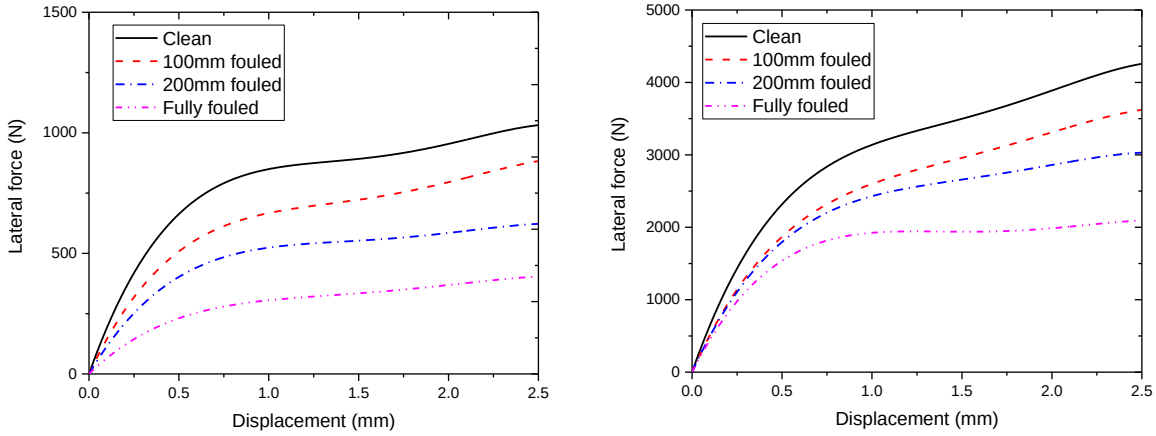

(a) Concrete sleeper with no ballast shoulder (b) Concrete sleeper with ballast shoulder

Figure 12. Lateral force – displacement graph for concrete sleeper considering fouled ballast.

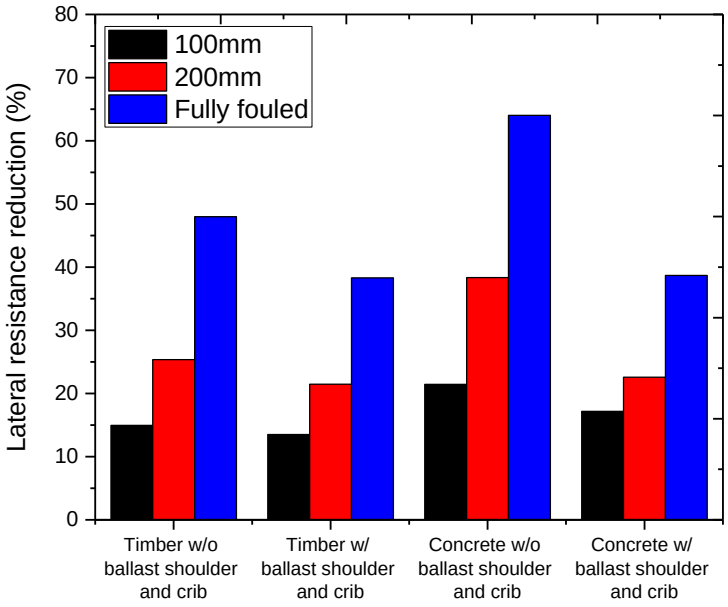

Figure 13. Lateral resistance reduction due to ballast fouling.

Figure 14 presents the lateral resistance contribution of each frictional component. The results are derived from the case when sleeper is placed on ballast bed with ballast crib and ballast shoulder. Note that the contributions are provided by sleeper base, ballast crib, and ballast shoulder as previously presented in Figure 4 and they are calculated from the percentage ratio of the component resistance to the total resistance ($\frac{R_{component}}{R_{total}} x100$). In Figure 14, the contributions were computed when the displacement of the sleeper was equal to 2mm. As for the timber sleeper, the percentage rations are 37-47% for the sleeper base, 20-34% for the ballast crib and 30-40% for the ballast shoulder. Whereas the sleeper base plays a higher percent contribution for ballasted track with the concrete sleeper and the percentage ratios are 56-68% for the sleeper base, 20-28% for the ballast crib and 12-16% for the ballast shoulder. This is because the concrete sleeper has a greater weight and larger dimensions resulting in

higher normal forces and frictional resistance at the base contact area. It is also noticeable that ballast crib of concrete sleeper case has a bigger contribution in lateral resistance than the ballast shoulder while it is less for the timber sleeper case. These results match well with the previous studies on the lateral resistance of ballasted track with concrete sleeper. Note that the boundary area in longitudinal direction of the rail was set as 600mm for both the timber and concrete sleeper cases. This slightly affects the number of ballast particles in the crib area as the number of ballast particles in contact with the concrete sleeper are probably fewer than that for the timber sleeper case due to the larger width of concrete sleeper. In accordance, the sleeper spacing also plays a role in the lateral resistance as it changes the contact with particles in crib ballast. Reducing the sleeper spacing can increase the lateral resistance due to ballast crib. In conclusion, the lateral resistance contributions provided by ballast in the crib and shoulder mainly depend on the ballast layer geometry and number of ballast particles in contact.

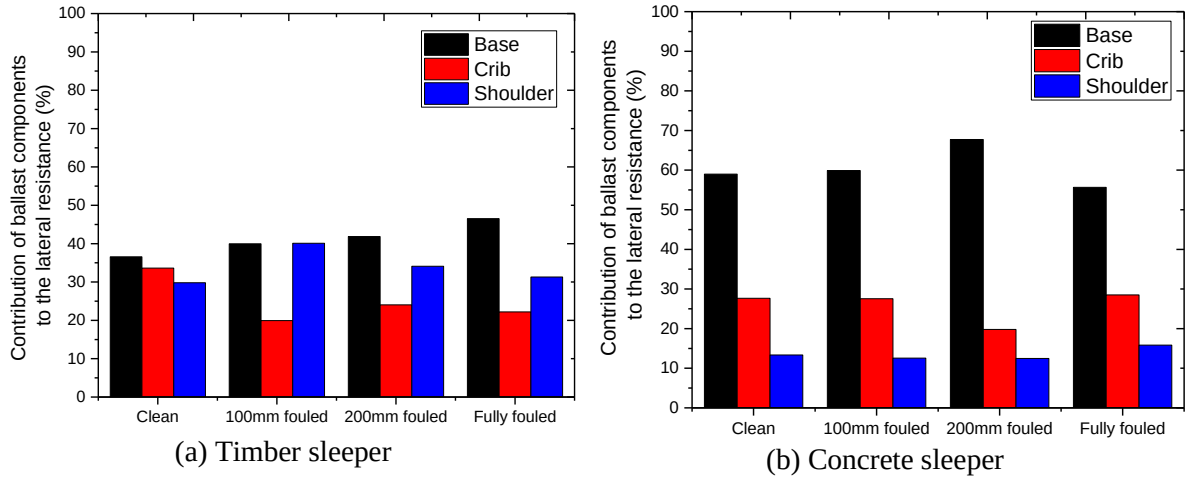

Figure 14. Contributions of different frictional components.

Figure 15 presents contact force distributions illustrating the force chains in the ballast layer of tracks and visualised for the different fouling conditions when the lateral displacement of sleeper reaches 2mm. The ballast layer contact forces are shown for the full longitudinal width of the ballast with no concern about ballast particles in the front obstructing the view of the ballast particles in the back. In this figure, the sleeper is pushed from left to the right. The darker and thicker areas represent the larger contact forces between particles while the lighter areas represent lesser ballast particle contact force. It should be noted that the larger contact force areas result in better support condition or resistance while the lighter areas represent insufficient support or poor resistance. In accordance, for all the cases analysed, the larger ballast contact forces are generated at the bottom of sleeper and near sleeper end while the ballast around crib area has less contact forces in comparison to ballast below the sleeper and ballast shoulder. The contact force chain intensities for the track with the timber sleeper, however, the contact forces are generally less than those for the concrete sleeper. Also, the clean ballast case has the highest contact forces between ballast particles and is followed by 100mm fouled, 200mm fouled and fully fouled, respectively, due to sleeper movement. This trend can be seen in a similar fashion for both the timber and concrete sleeper cases. In other words, the more severe are the fouling conditions, the lesser are the contact forces, and the ballast particles provide relatively lower lateral resistance for the sleeper movement. In summary, when ballast is degraded and fouling starts to accumulate from bottom up, the ballast support becomes much less sufficient to provide the needed lateral restraint to arrest the movement of sleeper.

Clean ballast

100mm fouled ballast

200mm fouled ballast

Fully fouled ballast

(a)

Clean ballast

100mm fouled ballast

200mm fouled ballast

Fully fouled ballast

(b)

Figure 15. Contact force chains of ballast layer with different conditions: (a) timber sleeper and (b) concrete sleeper.

5. Conclusions

This study focused on conducting ballasted track numerical simulations using the Discrete Element Method (DEM) to study Single Sleeper (Tie) Push Tests (STPTs), which essentially are performed in the field to quantify track lateral resistance associated with new clean and degraded (or fouled) ballast conditions. The result of ballast breakdown and fouling with usage on track lateral vulnerability has not been fully investigated in the past. Previous studies which considered coal dust filling the voids of new ballast layers could be modelled successfully in DEM simulations by adjusting the surface friction angle related to the ballast particle contacts. In a similar fashion, the fouled ballast layer conditions were created by adopting DEM model parameters, which have been calibrated previously against the direct shear and triaxial tests, to indicate each particle interaction has less friction when ballast layer is fouled.

In the DEM simulations of STPTs in this study, fouling was considered to start from the bottom of the ballast layer in different zones and was applied all the way to the top to represent the completely fouled ballast layer condition. Both timber and concrete sleepers were considered with proper weights and geometries in the simulations. Note that the sleeper base plays a significant role in lateral resistance especially for heavier and larger concrete sleepers.

The DEM simulation results in general matched well with findings from previous studies; ballast bed and crib had more contribution than ballast shoulder for concrete sleeper. However, for timber sleeper, ballast shoulder had higher influence than ballast crib due to the smaller width of sleeper. The DEM simulation results showed that ballast fouling significantly reduced the lateral resistance of ballasted track by up to about 48% for timber sleepers and 64% for concrete sleepers. In accordance, a depth profile fouling investigation of the ballast layer is therefore very important as ballast fouling conditions, often unseen or noticed from the ballast surface, can undermine the lateral stability of railway track. This may shift the buckling failure mode from snap-through to progressive buckling, due to the reduction in lateral resistance in the same track profile, and increase the risk of track buckling. The results can be used further for the full track buckling analysis to potentially evaluate the buckling temperature and phenomena of railway track under these conditions. The insights will enhance the inspection of lateral stiffness in railway systems and mitigate the risk of delays due to unplanned maintenance, thus paving a robust pathway for improved safety and a practical impact on societies.

Acknowledgments

The authors are sincerely grateful to European Commission for the financial sponsorship of the H2020-MSCA-RISE Project No. 691135 RISEN: Rail Infrastructure Systems Engineering Network, which enables a global research network that tackles the grand challenge in railway infrastructure resilience and advanced sensing in extreme environments (www.risen2rail.eu) [47].

References

1. Quinn A, Jack, A.; Hodgkinson, S.; Ferranti, E., Beckford J., Dora J. RAIL ADAPT Adapting the railway for the future. International Union of Railways (UIC); 2017.
2. Dindar S, Kaewunruen S, An M, Mohd O. Natural Hazard Risks on Railway Turnout Systems. Procedia Engineering 2016;161:1254–9.
3. Kaewunruen S, Wang Y, Ngamkhanong C. Derailment-resistant performance of modular composite rail track slabs. Engineering Structures. 2018;160:1-11.
4. Sussmann TR, Ruel M, Chrismer SM. Source of Ballast Fouling and Influence Considerations for Condition Assessment Criteria. Transportation Research Record: Journal of the Transportation Research Board. 2012;2289(1):87-94.
5. Anbazhagan P, Bharatha TP, Amarajeevi G. Study of Ballast Fouling in Railway Track Formations. Indian Geotechnical Journal. 2012;42(2):87-99.
6. Lei X, Feng Q. Analysis of stability of continuously welded rail track with finite elements. Proceedings of the Institution of Mechanical Engineers, Part F: Journal of Rail and Rapid Transit. 2004;218(3):225–33.

7. Carvalho J, Delgado J, Calçada C, Delgado R. A new methodology for evaluating the safe temperature in continuous welded rail tracks. International Journal of Structural Stability and Dynamics 2013;13(2):1350016.
8. Ngamkhanong C, Wey CM, Kaewunruen S. Buckling Analysis of Interspersed Railway Tracks. Appl Sci. 2020;10:3091.
9. European Rail Research Institute Committee D202. Improved knowledge of forces in CWR track (including switchws). Utrecht, Netherlands: European Rail Research Institute 1995.
10. Kish A. On the Fundamentals of Track Lateral Resistance. Annual Conference; 18-21 September; Minneapolis, USA2011.
11. American Railway Engineering and Maintenance-of-Way Association. Manual for Railway Engineering. 2004.
12. Nguyen VH, Duhamel D, Nedjar B. A continuum model for granular materials taking into account the no-tension effect. Mechanics of Materials. 2003;35(10):955-67.
13. Zakeri JA, Esmaeili M, Kasraei A, Bakhtiary A. A numerical investigation on the lateral resistance of frictional sleepers in ballasted railway tracks. Proceedings of the Institution of Mechanical Engineers, Part F: Journal of Rail and Rapid Transit. 2014;230(2):440-9.
14. Kabo E. A numerical study of the lateral ballast resistance in railway tracks. Proceedings of the Institution of Mechanical Engineers, Part F: Journal of Rail and Rapid Transit. 2006;220(4):425-33.
15. Ngamkhanong C, Kaewunruen S, Baniotopoulos C. A review on modelling and monitoring of railway ballast. Structural Monitoring and Maintenance. 2017;4(3):195-220.
16. Cundall PA. A Computer Model for Simulating Progressive, Large Scale Movements in Blocky Rock Systems. International Symposium on Rock Fracture; Nancy, France1971.
17. Huang H. Discrete Element Modeling of Railroad Ballast Using Imaging Based Aggregate Morphology Characterization [PhD Thesis]: University of Illinois at Urbana-Champaign; 2010.
18. González JI. Numerical modelling of railway ballast using the discrete element method [Master Thesis]: Escola de Camins; 2015.
19. Khatibi F, Esmaeili M, Mohammadzadeh S. DEM analysis of railway track lateral resistance. Soils and Foundations. 2017;57(4):587-602.
20. Jing G, Aela P, Fu H, Yin H. Numerical and experimental analysis of single tie push tests on different shapes of concrete sleepers in ballasted tracks. Proceedings of the Institution of Mechanical Engineers, Part F: Journal of Rail and Rapid Transit. 2018;233(7):666-77.
21. Guo Y, Fu H, Qian Y, Markine V, Jing G. Effect of sleeper bottom texture on lateral resistance with discrete element modelling. Construction and Building Materials. 2020;250.
22. Jing G, Aela P, Fu H. The contribution of ballast layer components to the lateral resistance of ladder sleeper track. Construction and Building Materials. 2019;202:796-805.
23. Xiao H, Ling X. Experiment and DEM Analysis of Lateral Resistance of Glued Ballast. Xinan Jiaotong Daxue Xuebao/Journal of Southwest Jiaotong University. 2017;52(6):1046-54.
24. Jing G, Zhang X, Jia W. Lateral resistance of polyurethane-reinforced ballast with the application of new bonding schemes: Laboratory tests and discrete element simulations. Construction and Building Materials. 2019;221:627-36.
25. Tutumluer E, Huang H, Hashash YMA, Ghaboussi J. Aggregate shape effects on ballast tamping and railroad track lateral stability. AREMA conference; USA2006.
26. Guo Y, Markine V, Song J, Jing G. Ballast degradation: Effect of particle size and shape using Los Angeles Abrasion test and image analysis. Construction and Building Materials. 2018;169:414-24.
27. Lichtberger B. The lateral resistance of the track. European Railway Review. 2007:68-71.
28. Feng B, Hou W, Tutumluer E. Implications of Field Loading Patterns on Different Tie Support Conditions using Discrete Element Modeling: Dynamic Responses. Transportation Research Record: Journal of the Transportation Research Board. 2019;2673(2):509-20.
29. Hou W, Feng B, Li W, Tutumluer E. Evaluation of Ballast Behavior under Different Tie Support Conditions using Discrete Element Modeling. Transportation Research Record: Journal of the Transportation Research Board. 2018;2672(10):106-15.
30. Jing G, Aela P. Review of the lateral resistance of ballasted tracks. Proceedings of the Institution of Mechanical Engineers, Part F: Journal of Rail and Rapid Transit. 2020;234(8):807-20.

31. Le Pen LM, Powrie W. Contribution of Base, Crib, and Shoulder Ballast to the Lateral Sliding Resistance of Railway Track: A Geotechnical Perspective. Proceedings of the Institution of Mechanical Engineers, Part F: Journal of Rail and Rapid Transit. 2011;225(2):113-28.
32. Zakeri JA, Mirfattahi B, Fakhari M. Lateral resistance of railway track with frictional sleepers. Proceedings of the Institution of Civil Engineers - Transport. 2012;165(2):151-5.
33. Zakeri JA, Bakhitiary A. Experimental investigation on effects of frictional sleeper in lateral resistance of railway tracks. Trans Res J (TRJ). 2013;10:159-69.
34. Zakeri JA, Mirfattahi B. Field investigation on the lateral resistance of railway tracks with frictional sleepers IOP Conf Series: Materials Science and Engineering. 2020;671.
35. Esmaeili M, Nouri R, Yousefian K. Experimental comparison of the lateral resistance of tracks with steel slag ballast and limestone ballast materials. Proceedings of the Institution of Mechanical Engineers, Part F: Journal of Rail and Rapid Transit. 2016;231(2):175-84.
36. Sussmann TR, Ruel M, Chrismer SM. Source of ballast fouling and influence considerations for condition assessment criteria. Transportation Research Record2012. p. 87-94.
37. Federal Railroad Administration. Heavy Axle Load Revenue Service Mudfouled Ballast Investigation. U.S. Department of Transportation; 2011 May 2011.
38. Moaveni M, Wang S, Hart JM, Tutumluer E, Ahuja N. Evaluation of Aggregate Size and Shape by Means of Segmentation Techniques and Aggregate Image Processing Algorithms. Transportation Research Record. 2013;2335(1):50-9.
39. Ghaboussi J, Barbosa R. Three-dimensional discrete element method for granular materials. International Journal for Numerical and Analytical Methods in Geomechanics. 1990;14(7):451-72.
40. Zhao D, Nezami EG, Hashash YMA, Ghaboussi J. Three-dimensional discrete element simulation for granular materials. Eng Comput 2006;23(7):749-70.
41. Huang H, Tutumluer E. Discrete Element Modeling for fouled railroad ballast. Construction and Building Materials. 2011;25(8):3306-12.
42. Selig ET, Waters JM. Track geotechnology and substructure management. London, UK1994.
43. Tennakoon N, Indraratna B, Nimbalkar S. Impact of ballast fouling on rail tracks. International Conference on Railway Technology: Research, Development and Maintenance Scotland: Civil-Comp Press; 2014.
44. Danquah WO, Ghataora GS, Burrow MPN. The effect of ballast fouling on the hydraulic conductivity of the rail track substructure. XV Danube - European Conference on Geotechnical Engineering (DECGE 2014); 9-11 September 2014; Vienna, Austria2014.
45. Indraratna B, Su LJ, Rujikiatkamjorn C. A new parameter for classification and evaluation of railway ballast fouling. Canadian Geotechnical Journal. 2011;48(2):322-6.
46. Huang H, Tutumluer E, Dombrow W. Laboratory Characterization of Fouled Railroad Ballast Behavior. Transportation Research Record: Journal of the Transportation Research Board. 2009;2117(1):93-101.
47. Kaewunruen S, Sussman JM, Matsumoto A. Grand Challenges in Transportation and Transit Systems. Frontiers in Built Environment. 2016;2(4).